

Au 6×6 ON Si(111): EVIDENCE FOR A 2D PSEUDOGLASS

L. D. MARKS and D. GROZEA

*Department of Materials Science and Engineering, Northwestern University,
Evanston, IL 60208, USA*

R. FEIDENHANS'L and M. NIELSEN

*Department of Solid State Physics and Chemistry, Risø National Laboratory,
DK-4000 Roskilde, Denmark*

R. L. JOHNSON

*II. Institute for Experimental Physics, University of Hamburg,
22761 Hamburg, Germany*

Received 10 October 1997

The atomic structure of the Au 6×6 on Si(111) phase has been determined using direct methods and surface X-ray diffraction data. This surface structure is very complicated, with 14 independent gold atoms, relaxations in 24 independent silicon sites and three partially occupied gold sites. In one sense the structure can be described as microdomains of the parent $\sqrt{3} \times \sqrt{3}$ Au on Si(111) structure. A better description is in terms of a tiling of incomplete pentagonal and trimer units, essentially a pseudopentagonal glass. In terms of these structural units it appears possible to explain all the gold structures in the coverage range of 0.8–1.5 monolayers as pseudoglasses with strong short range order but varying degrees of long range order.

The gold on Si(111) surface in the coverage range of 0–2 monolayers (ML) has been extensively studied, but many of the details are still unclear and the underlying physics uncertain. Below 1 ML two distinct phases, the 5×2^1 and $\sqrt{3} \times \sqrt{3}^2$ structures, are known to exist. Both of these are stable to temperatures far in excess of the bulk eutectic melting point of 363°C. In the range of 1.0–1.5 ML (and perhaps with slightly lower coverages), diffraction experiments show strong $\sqrt{3} \times \sqrt{3}$ intensities and additional diffuse or ordered structures.^{3–8} The best defined of these is the Au 6×6 structure at around 1.4 ML coverage which forms very close to the bulk eutectic temperature. At higher coverages gold particles form, probably Stranski–Krastanov growth.^{9,10} It should be noted that quenching the bulk eutectic is known to produce a glass¹¹ which appears to crystallize at similar temperatures into a number of yet poorly determined phases.^{12–14} Furthermore, there is some evidence from XPS¹⁵ and diffraction^{16,17} for a gold-silicide.

Understanding the Au 6×6 structure can shed light on the transition from a 2D surface to a more bulklike behavior. Furthermore, because the temperatures are very close to the bulk eutectic and glass formation/crystallization temperatures, unusual phenomena may be present. For instance, in this temperature/coverage range strong homoepitaxial growth of silicon has been observed.¹⁸ A previous attempt to look at this surface using X-ray diffraction data and a Patterson approach was at best only partially successful.⁴ STM studies indicate, at a gold coverage slightly above 1 ML, sets of three maxima surrounded by triangular domain walls and a number of bright “protrusions.”¹⁹ At a higher coverage (1.4 ML), another STM paper⁸ suggested a slightly different structure — a rectangular array of protrusions with a smaller periodicity than the 6×6 unit cell.

We have recently shown that direct methods can be used to solve surface structures.^{20–24} We report here their use to determine the atomic structure of

the Au 6×6 surface.

Details of the collection of the X-ray intensity data have been previously reported⁴ and will not be described herein. A total of 139 independent intensities in $p6mm$ and 248 for a plane group of $p3$ were used. For the direct methods we used a minimum entropy unitary Sayre method coupled with a genetic algorithm for global optimization, more details of which are given elsewhere.^{23,24} In essence, the approach finds the most ordered charge density maps consistent with the experimental intensities; the output is a number of plausible solutions with a robust likelihood for each. With small experimental measurement errors, a complete set of intensities and little nonkinematical scattering (for example from subsurface strains), these maps will be rather accurate reconstructions of the two-dimensional charge density. More often, only part of the structure will be identified in the initial analysis, the case herein.

Working from such an initial fragment, the full structure was determined by combining iterative steps of refinement (of the atomic positions) and heavy atom holography¹ to determine new sites. For reference, in $p3$ symmetry incoherent twin domains were assumed yielding $p6mm$ Patterson symmetry.

Shown in Fig. 1 is an initial fragment with about 20 gold atoms, found among the top solutions using $p3$ symmetry. While not obvious in the initial stages of the analysis, all the top solutions in both $p3$ and $p31m$ symmetry showed 20 or more of the gold atoms. Building from this structure we were able to generate the gold framework shown in Fig. 2, a total of 14 independent sites (42 atoms without the partially occupied sites). In terms of an R factor defined as

$$R = \sum \frac{|I_{\text{calc}}(h, k) - I_{\text{expt}}(h, k)|}{\sum I_{\text{expt}}(h, k)}$$

and reduced χ^n as

$$\chi^n = \frac{1}{M - N} \sum \left| \frac{I_{\text{calc}}(h, k) - I_{\text{expt}}(h, k)}{\sigma(h, k)} \right|^n, \quad (1)$$

with M data points each with errors $\sigma(h, k)$ and N variables, this structure gave $R = 0.25$ and $\chi^2 = 50$. While the χ^2 is rather high, it is more than two orders of magnitude better than that found in a previous analysis.²⁵ A strong possibility exists that the experimental results were obtained from a two-phase $\sqrt{3} \times \sqrt{3}$ and 6×6 mixture; eliminating reflections

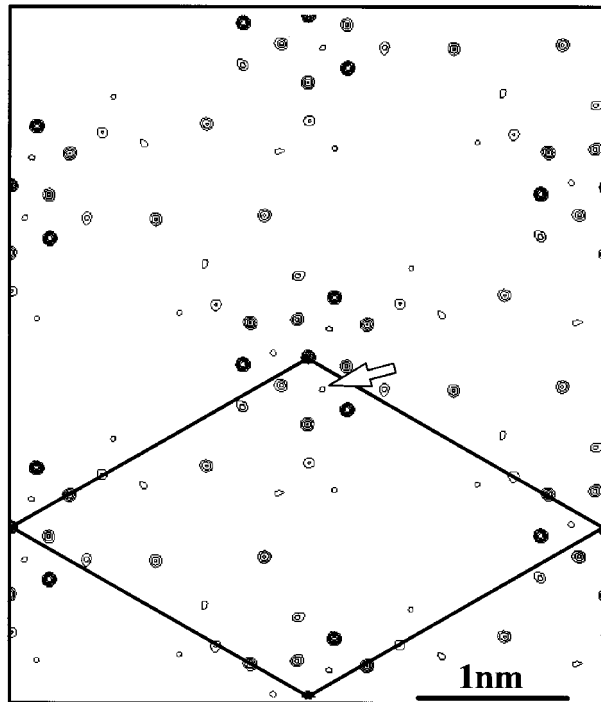


Fig. 1. Contour map of the initial fragment first used with the primitive unit cell indicated by solid lines and excluding negative contours. Including the peak at the origin which turned out to be only partially occupied, the peaks are very close to gold positions in the final refinement, and three weaker silicon peaks are observable. One of the three symmetry-equivalent Si peaks is arrowed; all the other peaks corresponds to Au sites. Other maps showed different fragments of the total structure.

which overlap with the $\sqrt{3} \times \sqrt{3}$ reduced χ^2 to about 32 and R to 0.2. (This reduced only slightly the number of reflections, from — in $p3$ — 248 to 234.) Adding a single silicon layer reduced these again by about a factor of 2; similarly a second silicon layer reduced χ^2 to about 8. Based upon previous work² with the $\sqrt{3} \times \sqrt{3}$, the relaxation extends several layers into the substrate. However, in $p3$ symmetry there are only 234 reflections (about half of these independent), so including large numbers of silicon atoms (12 per layer) is not justifiable in terms of the number of measurements. To compensate for not including all subsurface atoms, the more robust form χ was used. [This corresponds to $n = 1$ in Eq. (1), and is less sensitive to outliers in the data.] For one layer of silicon we obtained $\chi = 2.7$; for two, $\chi = 2.0$. Including partial

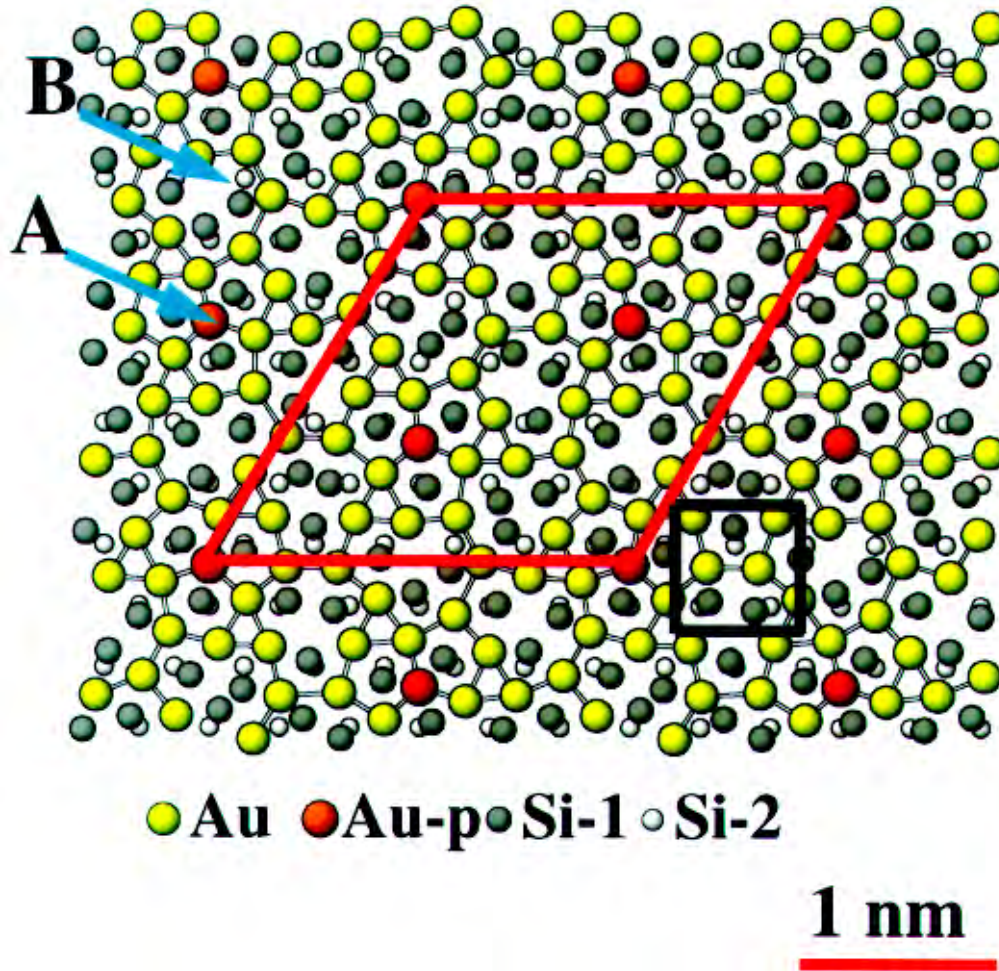


Fig. 2. Diagram of the structure, with the primitive unit cell indicated by solid lines and the notation Au-p for the partially occupied sites. The second layer silicon atoms are only slightly displayed from bulk sites — see Table I. The structure can be described in terms of incomplete pentagons and trimer units, or the two-gold-ring configurations A and B discussed in the text. One of the rectangular units observed in domain boundaries of the $\sqrt{3} \times \sqrt{3}$ structure is shown.

occupancy at the three special sites $(0, 0)$, $(1/3, 2/3)$ and $(2/3, 1/3)$ and expanding the subsurface strain field as the gradient of a two-dimensionally periodic harmonic^{26,27} had a large effect, yielding $\chi^2 = 3.8$ and $\chi = 1.7$, with a partial occupancy of approximately 0.5 (total coverage of 1.2 ML). For reference, no other solutions came close.

Atom positions for two silicon layers and some of the calculated and experimental intensity values are shown in Tables I and II respectively; for a more complete set see Ref. 25. For the atoms positions we averaged four calculations, two each using χ^2 and χ , with two different registries for the third layer of

silicon atoms, and then we used these to determine the errors. The gold site errors are about 0.01 \AA , the silicon about 0.05 \AA . However, since the gold Debye–Waller factor refined to a rather high value (0.16 \AA RMS displacement) implying substantial static disorder (consistent with partial occupancy), a multiplicative factor of 2–3 on the errors might be appropriate. Most of this is almost certainly rotation of the gold trimers, similar to the $\sqrt{3} \times \sqrt{3}$.² We were not able to refine the surface silicon Debye–Waller term, which tended to drop to unreasonable values, implying more subsurface relaxations than can be matched with the available data.

Table I. Average atomic positions with 14 gold sites and two Si layers (24 sites). Only two-dimensional diffraction data were available, so no heights could be refined. Values for the errors ($\delta X, \delta Y$) as well as the displacements from bulk sites for the subsurface silicon atoms ($\Delta X, \Delta Y$) are given.

Gold sites:					
X	δX		Y	δY	
0.3435	(0.0012)		0.8670	(0.0005)	
0.3090	(0.0005)		0.3018	(0.0002)	
0.1852	(0.0006)		0.1804	(0.0011)	
0.8647	(0.0004)		0.3488	(0.0003)	
0.2545	(0.0005)		0.0315	(0.0008)	
0.4470	(0.0007)		0.3553	(0.0005)	
0.9560	(0.0003)		0.0926	(0.0007)	
0.6276	(0.0003)		0.2048	(0.0005)	
0.4712	(0.0004)		0.8840	(0.0005)	
0.0089	(0.0006)		0.3582	(0.0001)	
0.2501	(0.0003)		0.7164	(0.0015)	
0.7832	(0.0003)		0.8687	(0.0002)	
0.4523	(0.0008)		0.2356	(0.0007)	
0.5880	(0.0004)		0.8725	(0.0003)	
Silicon layer 1:					
X	δX	$\Delta X(\text{\AA})$	Y	δY	$\Delta Y(\text{\AA})$
0.0309	(0.0021)	-0.569	0.9320	(0.0026)	-0.286
0.4116	(0.0009)	0.524	0.6237	(0.0014)	0.291
0.7445	(0.0014)	0.512	0.3147	(0.0032)	0.850
0.3681	(0.0024)	0.478	0.1072	(0.0006)	-0.090
0.3577	(0.0043)	-0.719	0.2350	(0.0021)	-0.985
0.2369	(0.0036)	0.338	0.1390	(0.0083)	0.643
0.1960	(0.0031)	-0.604	0.3002	(0.0042)	0.517
0.1738	(0.0024)	-1.115	0.3970	(0.0017)	-1.093
0.0908	(0.0008)	0.812	0.3398	(0.0021)	1.428
0.5261	(0.0001)	-0.679	0.4502	(0.0008)	0.133
0.5798	(0.0049)	0.558	0.5665	(0.0049)	-1.027
0.3955	(0.0010)	0.152	0.4152	(0.0015)	-0.674
Silicon layer 2:					
X	δX	$\Delta X(\text{\AA})$	Y	δY	$\Delta Y(\text{\AA})$
0.0582	(0.0002)	0.060	0.1099	(0.0007)	-0.028
0.2220	(0.0004)	-0.005	0.6090	(0.0001)	-0.049
0.7198	(0.0001)	-0.056	0.4453	(0.0012)	0.019
0.2249	(0.0006)	0.061	0.1144	(0.0002)	0.076
0.3882	(0.0007)	-0.015	0.1113	(0.0007)	0.004
0.3870	(0.0010)	-0.044	0.2756	(0.0006)	-0.050
0.0570	(0.0002)	0.033	0.2832	(0.0006)	0.125
0.2211	(0.0002)	-0.027	0.2794	(0.0007)	0.038
0.2189	(0.0001)	-0.077	0.4392	(0.0007)	-0.122
0.3926	(0.0007)	0.086	0.4408	(0.0008)	-0.083
0.5545	(0.0014)	-0.024	0.4469	(0.0015)	0.057
0.5591	(0.0010)	0.081	0.6086	(0.0010)	-0.057

The most interesting aspects of the structure is that it is astonishingly simple, and at the same time complicated. There is a strong relationship to the parent $\sqrt{3} \times \sqrt{3}$ with three sets of three gold trimers. More interesting is the structure of the additional gold atoms which form incomplete pentagons and trimer units; if all the special sites were occupied, complete pentagons would be formed. Every gold-gold separation is close to 0.28 nm, the bulk gold interatomic distance. At the center of these incomplete pentagons, probably at the lower apex of a pentagonal prism, are the silicon atoms of the next layer. In a number of cases silicon atoms are separated by 0.2 nm, implying the presence of second layer dimerization.

The correspondence at a qualitative level between the structure and the STM images^{8,19,28} at lower coverages is good. Similar to the parent $\sqrt{3} \times \sqrt{3}$, the trimers are not properly resolved, and the protrusions are the partially occupied special sites — these match the STM images not only in location within the unit cell but also in terms of their local symmetry. The overall symmetry of the structure is close to p31m, again matching well the STM images. The trimers are arranged in rectangular arrays (Fig. 2) which have previously been observed in the domain walls in the $\sqrt{3} \times \sqrt{3}$ structure, where they become more abundant with increasing coverage⁸ and the $\sqrt{3} \times \sqrt{3}$ LEED pattern more diffuse. This suggests that the domain walls in the $\sqrt{3} \times \sqrt{3}$ break up with increasing coverage and recognize as part of the 6×6 structure.

This structure is remarkably similar to what would be expected for a two-dimensional glass with pentagonal units, trimers and a rather fixed gold-gold separation. To understand this, note that the structure can be considered as a combination of the two Au ring structures A and B in Fig. 2 surrounding three silicon atoms in the next layer, with two rotational variants of B. Both rings sit at $\sqrt{3} \times \sqrt{3}$ lattice sites, the particular configuration shown giving the 6×6 structure; pure A units (with vacancies) will give the known $\sqrt{3} \times \sqrt{3}$ structure. Other tilings will yield a combination of trimers and incomplete pentagon units breaking the long range order to produce a glasslike structure. However, this would not be a true glass, because relatively sharp diffraction spots will be obtained at the $\sqrt{3} \times \sqrt{3}$ unit cell reciprocal lattice points, with diffuse scattering elsewhere

Table II. List of the intensities of the stronger reflections (using crystallographic notation, not fractional indices), the corresponding calculated values, the weighted error and absolute errors for $\chi^2 = 3.8$.

H	K	Expt.	Calc.	Wt. Err.	Abs. Err.
7	2	0.488E + 02	0.489E + 02	-0.330E - 01	-0.134E - 01
8	1	0.469E + 02	0.449E + 02	0.285E + 01	0.200E + 01
9	0	0.311E + 02	0.304E + 02	0.241E + 01	0.767E + 00
7	3	0.229E + 02	0.228E + 02	0.254E + 00	0.866E - 01
9	7	0.208E + 02	0.205E + 02	0.556E + 00	0.279E + 00
5	5	0.175E + 02	0.173E + 02	0.609E + 00	0.190E + 00
6	3	0.128E + 02	0.131E + 02	-0.132E + 01	-0.344E + 00
4	3	0.117E + 02	0.120E + 02	-0.183E + 01	-0.296E + 00
8	0	0.862E + 01	0.896E + 01	-0.132E + 01	-0.345E + 00
9	1	0.937E + 01	0.964E + 01	-0.995E + 00	-0.263E + 00
11	5	0.122E + 02	0.124E + 02	-0.608E + 00	-0.179E + 00
13	2	0.111E + 02	0.111E + 02	-0.580E - 01	-0.174E - 01
14	1	0.993E + 01	0.119E + 02	-0.303E + 01	-0.195E + 01
10	6	0.873E + 01	0.883E + 01	-0.462E + 00	-0.993E - 01
10	7	0.810E + 01	0.768E + 01	0.190E + 01	0.421E + 00
16	1	0.793E + 01	0.817E + 01	-0.595E + 00	-0.238E + 00
7	5	0.718E + 01	0.610E + 01	0.437E + 01	0.108E + 01
6	5	0.689E + 01	0.454E + 01	0.184E + 01	0.235E + 01
15	4	0.596E + 01	0.642E + 01	-0.118E + 01	-0.460E + 00
15	0	0.592E + 01	0.622E + 01	-0.922E + 00	-0.298E + 00
3	5	0.584E + 01	0.598E + 01	-0.599E + 00	-0.143E + 00

in agreement with experimental data.³⁻⁸ We hypothesize that the whole coverage range of 0.8–1.5 ML is really a surface solution pseudoglass. As such it is a two-dimensional analog of the bulk glassy state, which may well have similar structural units.

Many questions remain open about this structure. It would obviously be good to obtain more precise information about the silicon sites, which would require collection of a larger data set using either X-ray or transmission electron diffraction. (Electron diffraction will be more sensitive to the silicon sites.) We also suspect that there may be other ordered structures, and there is some evidence already for this from electron diffraction⁶ and STM data.⁸ Aside from the structural aspects, an intriguing question is the character of the electronic states in this two-dimensional structure. In addition to standard surface-spectroscopic techniques, matching the already available STM data at different biases with theoretical calculations would be very interesting.

Acknowledgments

This work was supported by the National Science Foundation (LDM and DG) on grant #DMR-9214505.

References

1. L. D. Marks and R. Plass, *Phys. Rev. Lett.* **75**, 2172 (1995) and references therein.
2. R. Plass and L. D. Marks, *Surf. Sci.* **342**, 233 (1995) and references therein.
3. K. Higashiyama, S. Kono and T. Sagawa, *Jpn. J. Appl. Phys.* **25**, L117 (1986).
4. D. Dornisch, W. Moritz, H. Schulz, R. Feidenhans'l, M. Nielsen, F. Grey and R. L. Johnson, *Phys. Rev.* **B44**, 11221 (1991).
5. S. Takahashi, Y. Tanashiro and K. Takayanagi, *Surf. Sci.* **242**, 73 (1991).
6. J. Yuhara, M. Inoue and K. Morita, *J. Vac. Sci. Technol.* **A10**, 334 (1992).
7. J. Yuhara, M. Inoue and K. Morita, *J. Vac. Sci. Technol.* **A10**, 3486 (1992).

8. T. Takami, D. Fukushi, T. Nakayama, M. Uda and M. Aono, *Jpn. J. Appl. Phys.* **33**, 3688 (1994).
9. G. Le Lay, G. Quentel, J. P. Faurie and A. Mason, *Thin Solid Films* **35**, 273 (1976).
10. W. Swiech, E. Bauer and M. Mundschau, *Surf. Sci.* **253**, 283 (1991).
11. W. K. Klement, R. H. Willens and P. Duwez, *Nature* **187**, 869 (1960).
12. H. Okamoto and T. B. Massalski, *Bull. Alloy Phase Diag.* **4**, 190 (1983).
13. W. Robinson, R. Sharma and L. Eyring, *Acta Metall. Mater.* **39**, 179 (1991).
14. F. H. Baumann and W. Schroter, *Phys. Rev.* **B43**, 6510 (1991).
15. A. Hiraki and M. Iwami, *Jpn. J. Appl. Phys. Suppl.* **2**, 749 (1974).
16. A. K. Green and E. Bauer, *J. Appl. Phys.* **47**, 1284 (1976).
17. A. Ichimiya, H. Nomura, Y. Ito and H. Iwashige, *J. Cryst. Growth* **150**, 1169 (1995).
18. G. D. Wilk, R. E. Martinez, J. F. Chervinsky, F. Spaepen and J. A. Golovchenko, *Appl. Phys. Lett.* **65**, 866 (1994).
19. J. Nogami, A. A. Baski and C. F. Quate, *Phys. Rev. Lett.* **65**, 1611 (1990).
20. L. D. Marks, R. Plass and D. Dorset, *Surf. Rev. Lett.* **4**, 1 (1997).
21. C. Collazo-Davila, L. D. Marks, K. Nishii and Y. Tanishiro, *Surf. Rev. Lett.* **4**, 65 (1997).
22. C. J. Gilmore, L. D. Marks, D. Grozea, C. Collazo-Davila, E. Landree and R. D. Twisten, *Surf. Sci.* **381**, 77 (1997).
23. E. Landree, C. Collazo-Davila and L. D. Marks, *Acta Cryst.* **B53**, 916 (1997).
24. L. D. Marks and E. Landree, *Acta Cryst. A*, in print.
25. An extended presentation of various analysis steps will be published elsewhere.
26. G. Jayaram, P. Xu and L. D. Marks, *Phys. Rev. Lett.* **71**, 3489 (1993).
27. A. E. H. Love, *A Treatise on the Mathematical Theory of Elasticity* (Dover, New York, 1994), p. 172.
28. J. Falta, A. Hille, D. Novikov, G. Materlik, L. Seehofer, G. Falkenberg and R. L. Johnson, *Surf. Sci.* **330**, L673 (1995).